GRAVITY AND GRANULAR MATERIALS

R.P. Behringer[1], Daniel Hovell[1], Lou Kondic[1], Sarath Tennakoon[1], Christian Veje[2]
[1]*Department of Physics and Center for Nonlinear and Complex Systems, Duke University, Durham NC, 27708-0305*
bob@ phy.duke.edu
[2]*Center for Chaos and Turbulence Studies, Niels Bhor Institute, Blegdamsvej 17, DK-2100 Copenhagen ø, Denmark*

We describe experiments that probe a number of different types of granular flow where either gravity is effectively eliminated or it is modulated in time. These experiments include the shaking of granular materials both vertically and horizontally, and the shearing of a 2D granular material. For the shaken system, we identify interesting dynamical phenomena and relate them to standard simple friction models. An interesting application of this set of experiments is to the mixing of dissimilar materials. For the sheared system we identify a new kind of dynamical phase transition.

I. INTRODUCTION

Granular flows exhibit a rich phenomenology [1] that is still only partially understood. On the Earth, granular materials show dynamics that is often dominated by the effects of gravity. For instance, they are typically random densely packed at rest; if they initially have a large kinetic energy, so that they are in a gas-like state, inelastic effects quickly dissipate that energy, leading back to the dense state. In a reduced gravity environment, the dynamics of granular materials is almost certainly different. The dense packed state is much less likely to occur, and other interesting phenomena are likely to be unmasked. For instance, in the present work, we have identified a second-order-like phase transition that is always masked by gravity for ordinary materials; this transition would be accessible in low gravity. Goldhirsch and Zanetti [2] have predicted that as a granular gas cools, it will undergo another dynamical transition that will lead to spatial inhomogeneity, although gravity makes the study and interpretation of this effect on earth difficult.

Understanding these phenomena would be scientifically interesting, and quite possibly technically important. Such understanding would be crucial in any effort to mine in a reduced gravity environment, such as the Moon.

In the experiments described below we have probed the effects of gravity in two ways. In the first, we have modulated gravity through shaking. In the second kind of experiment, we studied 2D granular systems where the "grains" slid on a smooth slippery surface that is horizontal. In this case, the surface carried the weight of the grains, and gravity played no role in setting the density of the grains. In the following two sections we highlight some of the recent results for each of these two types of experiments.

II. MODULATION OF GRAVITY BY SHAKING

Shaking provides a simple way of modulating gravity. Here, we vary gravity by shaking both in the vertical direction with a displacement

$$z = A_\upsilon \cos(\omega_\upsilon t), \qquad (1)$$

and in the horizontal direction with a displacement

$$x = A_h \cos(\omega_h t + \phi). \qquad (2)$$

The most important control parameters are then the dimensionless accelerations $\Gamma_i \equiv A_i \omega_i^2 / g$, where $i = h, \upsilon$.

For these experiments, we have developed a novel apparatus, Fig. 1, that allows us to provide independent 2-axis shaking (a third axis could be added in future experiments). An additional feature of the apparatus is that it allows us to fluidize the grains by gas flow through a porous bottom plate. This fluidization is intended to reduce the contact forces between grains, and also reduces the effect of gravity.

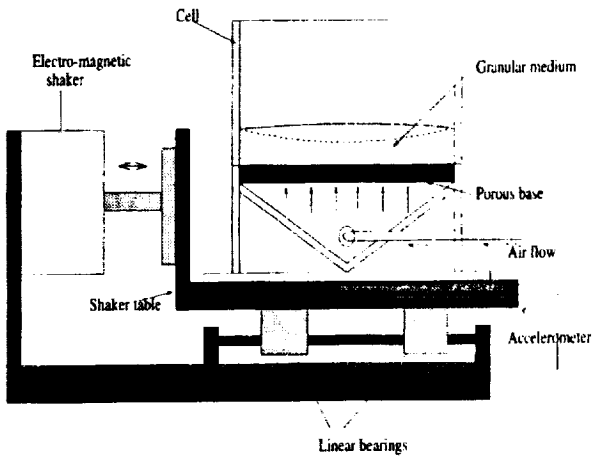

Figure 1: Schematic of the apparatus. The rectangular cell is made of Plexiglas, and is mounted on a Plexiglas base of the same cross-sectional dimensions which is attached to a small table. The table is mounted on four linear bearings running on horizontal cylindrical guidance rods rigidly attached to a fixed bottom frame. The bottom section of the cell acts as a gas distributor. An electro-mechanical actuator, driven by a sinusoidal AC signal provides the horizontal driving.

Gravity plays a crucial role in granular friction, since gravity is responsible for the compaction of virtually every earth-bound material. By modulating gravity, as in these experiments, we provide a useful probe of friction laws which date to the time of Coulomb, but are still only partially understood. The simple picture is that static friction provides a restraining shear force up to some maximum, $F_f = \mu F_N$, after which slipping, i.e. failure can occur. At failure, the friction coefficient falls to its kinetic value, μ_k.

For purely horizontal shaking, we have studied [3] the onset of flow as $\Gamma_h\Gamma$ is increased from 0. Key findings of this work are contained in Figs. 2 to Fig. 5. The initial transition to flow is hysteretic, i.e. once flow has begun at $\Gamma = \Gamma^*$, it can be sustained to lower $\Gamma = \Gamma_c$. The hysteresis is lifted, however, if the layer is dilated about 2% by gas fluidization. This amount of fluidization corresponds to an effective decrease of the weight of the grains of about 40%. We interpret this result to mean that the primary source of hysteresis comes from the friction at grain contacts, with possibly a less important contribution due to the interlocking of grains. Here, a key point is that in ordinary descriptions of granular friction, it is not possible to distinguish between the normal forces generated by the interlocking of grains, and the tangenial friction forces at grain contacts.

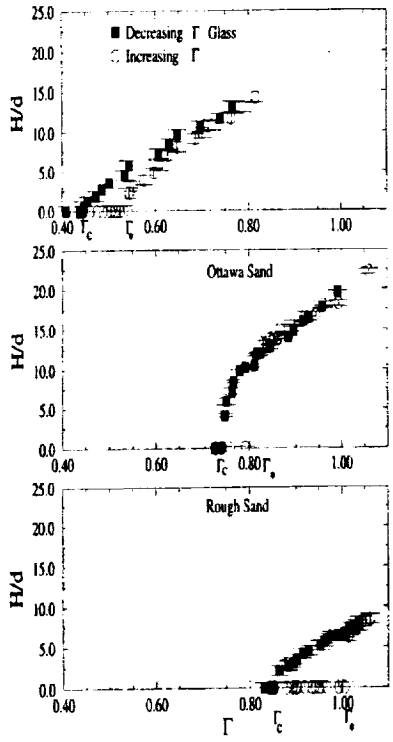

Figure 2: Height, ΓH of the fluidized layer vs. Γ_h for horizontal shaking. Data are for several materials, and show the hysteresis at onset. Flow begins at Γ^* and ceases with decreasing Γ at Γ_c.

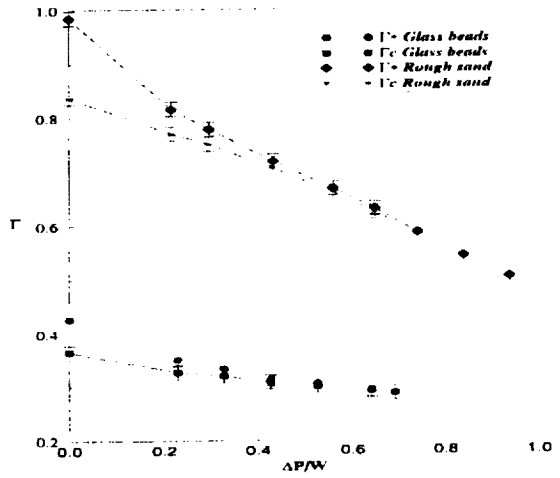

Figure 3: Data for Γ^* and Γ_c vs. gas levitation pressure in units of the weight per area of the material. For modest amounts of gas levitation, the hysteresis in the transition to flow is removed.

The overall flow pattern consists of sloshing motion which drives convection in the direction of shaking, plus a novel wall shearing effect that drives a weaker flow in the cross direction to shaking as well as downward at the sidewalls parallel to the shaking direction, Fig. 4.

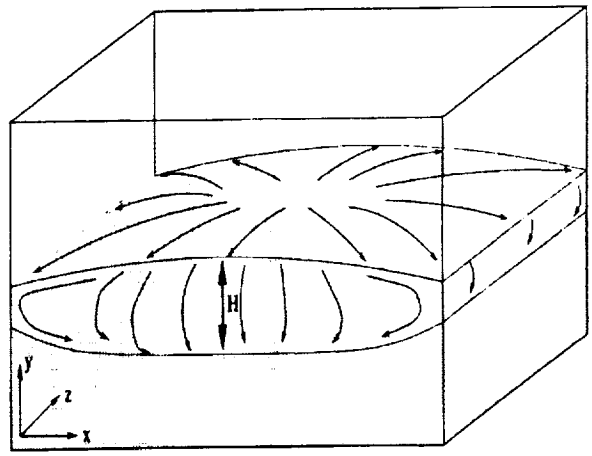

Figure 4: Sketch of time-averaged flow lines for horizontal shaking. The direction of shaking is the x-direction. H is the height of the flowing (fluidized) layer. The strongest flow consists of sloshing of the grains in the x-direction, with down flow at the endwalls, and corresponding inflow towards the center. There is also a shear-driven flow downward on average along the x-y bounding walls.

We have probed the latter effect through soft-particle MD simulations. These simulations are for 7000 particles interacting via a soft-particle simulation [5]. The downward motion at the sidewall occurs because of dilation near that wall from shearing. Hence, near this wall, grains have an enhanced mobility, and can fall under gravity. We expect that this mechanism would occur routinely when there is a shear layer plus gravity.

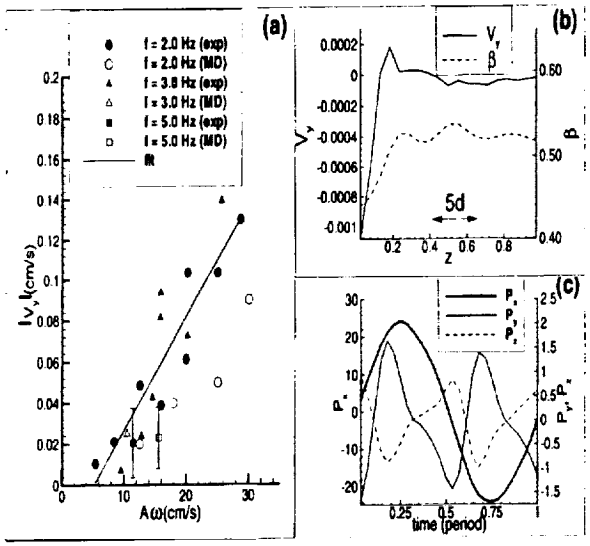

Figure 5: a) Experimental data (solid symbols) and MD simulations (open symbols) for shear-driven downward vertical velocity at the x-y walls vs. shaking velocity, $A_h\omega_h$. b) Velocity profile, V_y, obtained from MD simulations. c) MD simulations show complex structure over a shaking period for the mean value of the particle momentum.

For mixed vertical and horizontal shaking, a number of interesting effects occur [4], including the spontaneous formation of static heaps and at higher horizontal accelerations, the onset of sloshing flow. Static heaps form spontaneously at $\Gamma_h = \Gamma_{h1}$ when $\Gamma_v < 1$, and Γ_h is gradually increased from 0. Sloshing flow occurs at yet higher $\Gamma_h = \Gamma_{h2}$ when Coulomb friction can no longer sustain grains from sloshing up and down the inclined slope of the spontaneously formed heap.

Below, we describe recent results in the context of Fig. 6. We understand the formation of static heaps at the point at which grains become unstable to the horizontal acceleration under the reduced effective gravity $g(1 - \Gamma_v)$ that occurs as the shaker is accelerating downward. At the same time, if the shaker is driven horizontally in phase ($\phi = 0$) with the vertical motion, then the grains will slide until they reach the appropriate end wall. This process stops when a steep enough incline has developed, so long as Γ_h is not too large. However, if the Γ_h is large enough, slipping will occur for either direction of horizontal motion, and sloshing of the grains results. Standard Coulomb friction predicts all of these features qualitatively but not quantitatively. Specifically, we consider a simple model consisting of a block resting on an plane inclined at an angle θ and subject to uniform (i.e. non-oscillatory) accelerations of size $g\Gamma_v$ and $g\Gamma_h$ in the vertical and horizontal directions respectively. The block will first slide on a horizontal surface when $\Gamma_h = \mu(\Gamma_c - \Gamma_v)$ ($\Gamma_c = 1$), and we identify this event with the onset of static heap formation at Γ_{h1}, Fig. 7. We identify sloshing in the granular system with a Γ_{h2} such that the block would slide for either direction of horizontal shaking, Fig. 8. A comparison of the model and the experiment, even when Γ_c is allowed to be adjustable, shows that the model is only approximately correct.

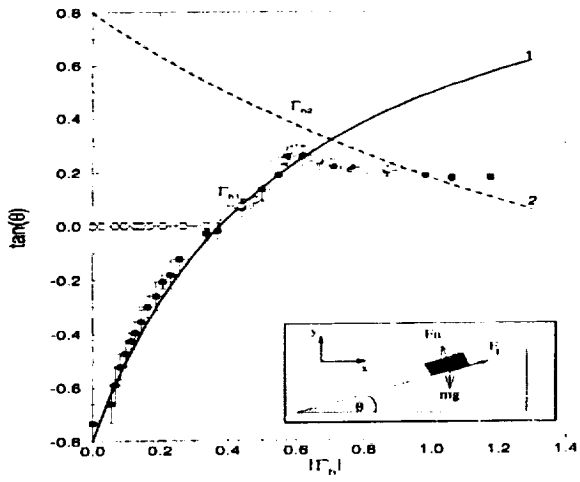

Figure 6: Data for the onset of flow under vertical and horizontal shaking. Here, Γ_v is held constant at 0.68. Open symbols are pertain to Γ_h increasing from 0, starting from a flat heap. Solid symbols pertain to a similar increase in Γ_h starting from a heap inclined at the ordinary angle of repose. Solid curves are derived from simple Coulomb friction, based on the sketch in the inset.

The shaker experiment provide several other interesting insights, although for space reasons, we do not provide extensive details here. One particularly interesting application of the shaking technique used here is for the mixing of dissimilar granular materials. Another system that we consider consists of a binary mixture of spheres that are identical except that some of the spheres have a higher coefficient of rolling friction than the other half. The spheres are then placed on a flat surface that is shaken horizontally. We find interesting segregation effects that we will describe elsewhere.

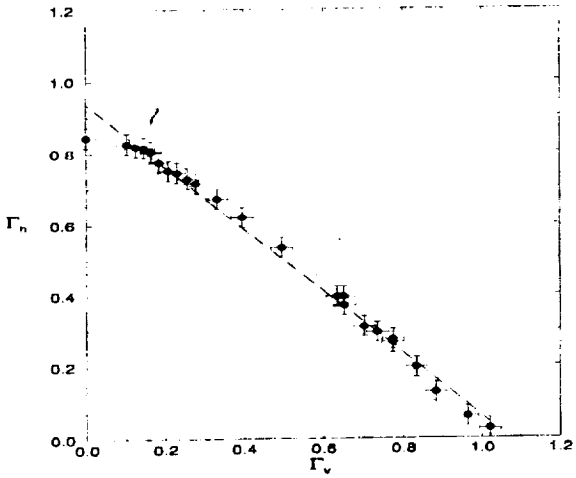

Figure 7: Comparison of data for the onset Γ_h vs. Γ_v for the spontaneous formation of a heap (Γ_1) and the simple Coulomb friction model – i.e. a straight line.

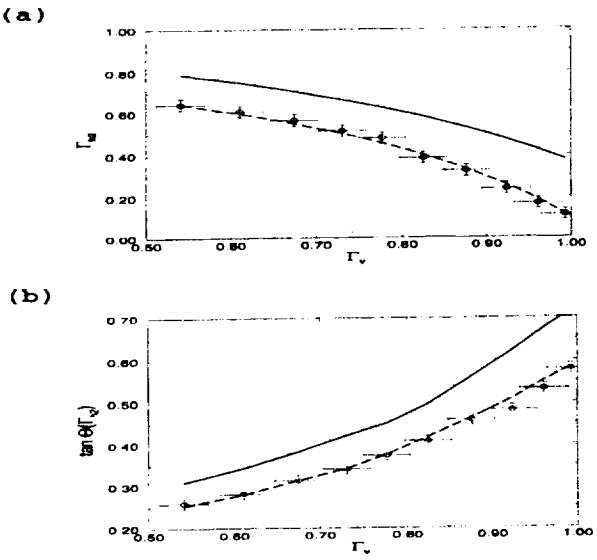

Figure 8: Data for Γ_{h2}, the onset of sloshing, and the angle of the heap at Γ_{h2} for $\Gamma_v = 0.68$. Solid curves are based on the predictions of a simple friction model.

The final experiment [6] consists of disks, a 2D granular material, that slide on a smooth slippery plane, and that are sheared in an annular geometry, Fig. 9. Specifically, the grains are sheared either by a rough inner wheel or by a surrounding rough outer ring. A key feature in these experiments is the absence of gravity, so that we can independently control the density. The disks are photoelastic, i.e. birefringent in proportion to the local deformation of the disks. We view them using a circular polariscope and use a novel technique to relate the photoelastic measurement to the applied force. In this technique, we exploit the fact that the transmitted light intensity, I depends locally on the local difference in the principle stresses with a disk. As the force at a contact increases, a series of light and dark bands appears within the disk, with the number of bands depending on the contact force. Hence, G, the gradient-square of $\Pi G = |\Delta G|^2$, integrated over a grain size gives a good measure of the number of bands, and hence of the local applied force. In addition, each disk is marked with a dark bar so that we can track individual particle positions and orientations using video. From these measurements we deduce particle velocities, V and rotation rates (spins), S. Here, we will focus on the velocity in the azimuthal direction, V_θ, where V_θ is the angular velocity of the grains. In addition, we measure the local packing fraction, γ, which is effectively the density of disks. Here, we will focus on shearing by the inner wheel only, although it is also possible to shear by the outer ring.

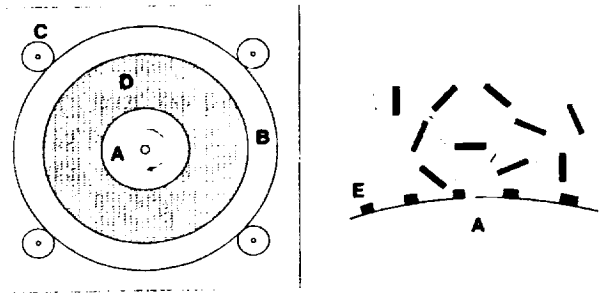

Figure 9: Sketch of 2D shear apparatus. Disks confined to a horizontal plane, and the region between wheel, A, and outer ring, B are steadily sheared by the wheel. The wheel is roughened by teeth, E, and have small dark bars for tracking purposes.

The figures below present some of the key results. Shearing by the inner wheel creates a shear band where the density (packing fraction, γ) is significantly reduced, Fig. 10, and where there is a nearly exponential variation of the mean azimuthal velocity, V_θ with distance, r/d, from the wheel, where d is the particle diameter (Fig. 11). In addition, the mean particle rotation rates, or spins, S show novel oscillations with distance from the wheel. There is a decreasing amount of dilation as γ increases. We observe approximate but not perfect rate invariance in the V_θ and S, as we change the wheel rotation rate, Ω, and we attribute the modest departures from rate invariance to small long time restructuring of the grains well away from the wheel.

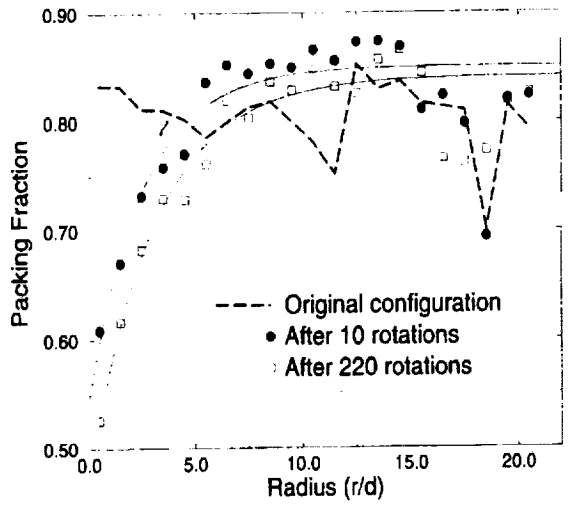

Figure 10: Packing fraction profile, γ vs. radial distance r/d (d = particle diameter) from the shearing wheel, showing the formation of a shear band.

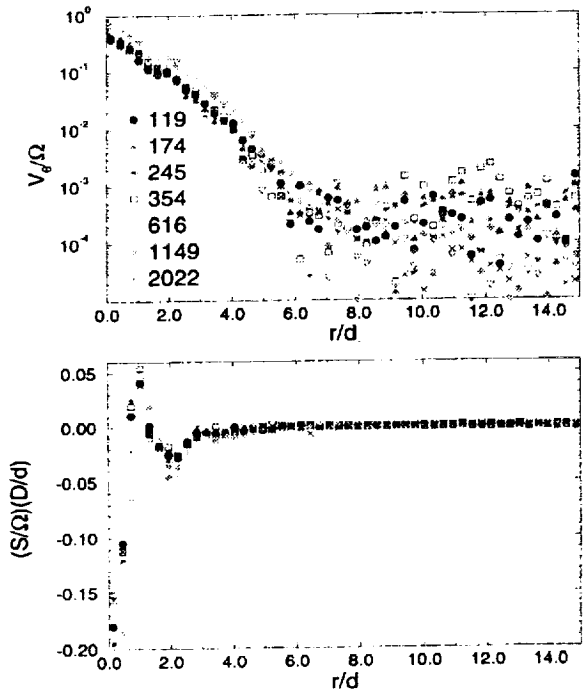

Figure 11: Mean azimuthal velocity, V_θ, and mean spin, S vs. distance r from the shearing wheel in units of a disk diameter, D. Data are for different wheel rotation rates, $\Omega = 2\tau/\tau$, where τ is the time in seconds for one wheel revolution. Data are normalized to test for rate invariance, i.e., kinematic quantities such as S or V_θ should be linearly proportion to Ω.

Distributions for V_θ and S are also quite interesting, Fig. 12. These show a combination of stick and slip motion for the particles nearest the wheel. As the packing fraction γ increase, there is transition from essentially complete slipping to nonslip with both rotation and translation of the disks.

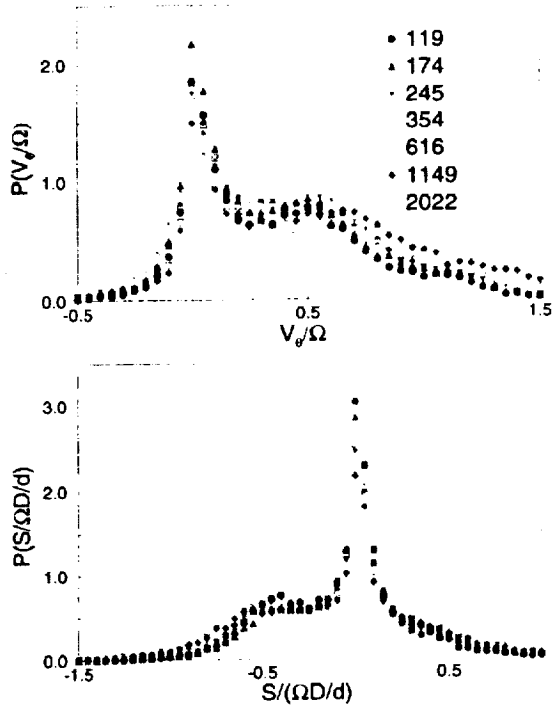

Figure 12: Examples of the distributions for azimuthal velocity and spin of particles next to the shearing wheel. The packing fraction is $\gamma = 0.788$ which is above the critical packing fraction.

A particularly interesting feature of these experiments is the observation of a transition at a critical packing fraction, γ_c, that has some of the hallmarks of a second order phase transition. Here, $\gamma - \gamma_c$ is the order parameter. At $\gamma_c \simeq 0.77$, the grains can just sustain shear, and the system is highly compressible. Also, there is critical slowing down: for instance the mean speed of the grains vanishes, Fig. 13. The distribution of forces changes qualitatively near γ_c. Well above γ_c, the distribution is qualitatively like the predictions of the q-model [7] of Coppersmith et al.: roughly exponential for large forces. Time series for the stress and the corresponding spectra are similar to these that we found for sheared 3D materials [8]. Specifically, for a give shear rate and γ, the spectrum typically varies as f^{-2} at high frequencies, f, and as a powerlaw, $P \propto f^{-\alpha}$ with $0 < \alpha < 1$. Nearer the transition, the distribution is qualitatively different, and ongoing

measurements will be characterize the distribution in that case. We observe an interesting and apparently smooth change from slip to nonslip behavior as we pass beyond γ_c.

Finally, if we define a slip event to be continuous decrease in the measured stress. Distributions of the size, M of slip events are exponentially distributed well above γ_c but appear to vary as M^{-1} for small M when γ is close to γ_c.

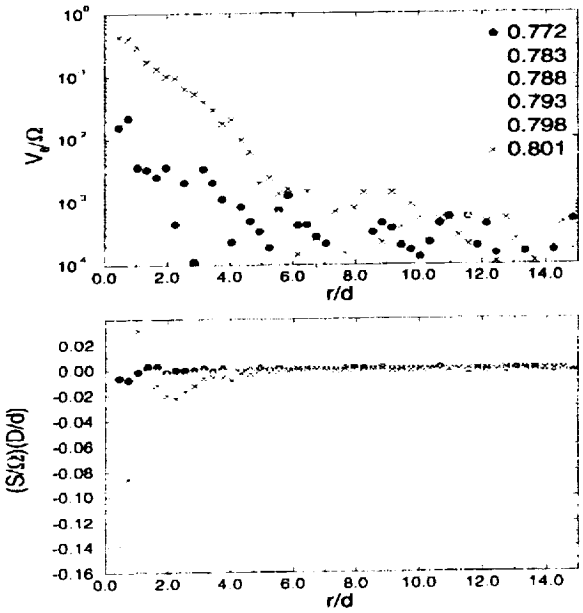

Figure 13: Mean azimuthal velocity and spin profiles for various packings fraction γ showing slowing down near as $\gamma - \gamma_c$ from above. We estimate that $\gamma_c = 0.77$ for this 2D system.

Acknowledgments. This work was supported by NASA grant NAG3-1917. We appreciate the hospitality of the P.M.M.H. of the Ecole Superieure de Physique et Chemie Industrielle de Paris, where parts of this work were carried out.

[1] For reviews see H.M. Jaeger, S.R. Nagel and R.P. Behringer, Rev. Mod. Phys. **68**, 1259 (1996); R.P. Behringer and J.T. Jenkins, ed. *Powders and Grains '97*, Balkema, Rotterdam (1997); H.J. Herrmann, S. Luding, and J.P. Hovi, eds. *Dry Granular Media*, NATO ASI series, Kluver, Amsterdam (1998).

[2] I. Goldhirsch and G. Zanetti, Phys. Rev. Lett. **70**, 1619 (1993).

[3] S. Tennakoon, L. Kondic, and R.P. Behringer, submitted to Phys. Rev. Lett. (1998).

[4] S. Tennakoon and R.P. Behringer, to appear, Phys. Rev. Lett. (1998).

[5] G.S. Grest and K. Kremer, Comp. Phys. Comm. **55**, 269 (1989); P.A. Thompson and G.S. Grest, Phys. Rev. Lett. **67**, 1751 (1991).

[6] D. Howell, B. Miller, C. O'Hern, and R.P. Behringer, in *Friction, Arching, Contact Dynamics*, p. 133-148, World Scientific (1997); C.T. Veje, D.W. Howell, and R.P. Behringer, S. Schollmann, S. Luding and H.J. Herrmann, in *Dry Granular Media*, eds. H.J. Herrmann, S. Luding, J.P. Hovi, Nato ASI series, Kluver, Amsterdam (1998).

[7] C.-h. Liu et al. *Science* **269**, 513 (1995); S.N. Coppersmith et al. Phys. Rev. E **53**, 4673 (1996).

[8] B. Miller, C. O'Hern, and R.P. Behringer, Phys. Rev. Lett. **77**, 3110 (1996).